

# Magnetohydrodynamic Power Generation in the Laboratory Simulated Martian Entry Plasma

L. Vušković<sup>1</sup>, S. Popović<sup>1</sup>, J. Drake<sup>1</sup> and R. W. Moses<sup>2</sup>

<sup>1</sup>*Old Dominion University, Department of Physics, Norfolk, VA*

<sup>2</sup>*NASA Langley Research Center, Hampton, VA*

**Abstract.** This paper addresses the magnetohydrodynamic (MHD) conversion of the energy released during the planetary entry phase of an interplanetary vehicle trajectory. The effect of MHD conversion is multi-fold. It reduces and redirects heat transferred to the vehicle, and regenerates the dissipated energy in reusable and transportable form. A vehicle on an interplanetary mission carries about 10,000 kWh of kinetic energy per ton of its mass. This energy is dissipated into heat during the planetary atmospheric entry phase. For instance, the kinetic energy of Mars Pathfinder was about 4220 kWh. Based on the loss in velocity, Mars Pathfinder lost about 92.5% of that energy during the plasma-sustaining entry phase that is approximately 3900 kWh. An ideal MHD generator, distributed over the probe surface of Mars Pathfinder could convert more than 2000 kWh of this energy loss into electrical energy, which correspond to more than 50% of the kinetic energy loss. That means that the heat transferred to the probe surface can be reduced by at least 50% if the converted energy is adequately stored, or reradiated, or directly used. Therefore, MHD conversion could act not only as the power generating, but also as the cooling process. In this paper we describe results of preliminary experiments with light and microwave emitters powered by model magnetohydrodynamic generators and discuss method for direct use of converted energy.

## Introduction

Motivation of this work is to validate the concept of magnetohydrodynamic power generation during the Martian probe entry phase. During the Martian probe entry phase, which lasts between 100 and 300 s, most of the probe's kinetic energy is converted into heat and thermal ionization. For instance, the total entry mass of Mars Pathfinder was 570 kg. Its entry velocity at 130 km was 7300 m/s. Therefore, its total kinetic energy before the entry phase was about  $1.52 \times 10^{10}$  J or 4220 kWh. This energy was lost into heat and released into the atmosphere during the Martian atmospheric (MA) entry of the probe.

Extraction and transfer of a part of the lost energy with the efficiency of 1% would result in 40 kWh of energy available for the equipment. This would increase more than two times the available instrument power of a landed probe for the period of 100 sols. Due to high degree of ionization in Martian entry plasma the MHD power extraction could be far more efficient.

Our goal in the present analysis was to set up a laboratory experiment in order to validate the concept and demonstrate the feasibility of MHD power extraction. We start our analysis with the Mars entry data, including the atmospheric composition, simplified models for altitudinal temperature, pressure and density distributions, compiled from the available Viking and Pathfinder data, and by an exemplary Martian probe trajectory, compiled from the actual Mars Pathfinder data.

## Model of MHD Power Conversion

In Figures 1-6 we present results of a simplified analysis and estimate of the MHD extracted power. The analysis is based on the actual Martian probe entry trajectory, and covers all necessary steps for the MHD power calculation, but in an approximate form. For instance, temperature and pressure in the boundary layer of the entry plasma were taken from simple jump conditions, without going into detailed analysis of the ionization in the shock layers. This analysis requires a developed of ionization recombination model of the MA entry plasma. Based on a simplified model of MSG plasma developed in this laboratory (Dinh, 2002) and on the thermodynamic parameters calculated from jump conditions, we obtained approximate gas composition of the MA entry plasma (see Figure 4). In the next

step electron density was evaluated on the basis of Saha equilibrium for the actual gas mixture, assuming that the electron and gas temperature equilibrate in the shock layer at about 60% of the original gas temperature obtained from the jump conditions. Thus the calculated altitudinal distribution of electron density levels is given in Figure 5. Based on the electron density distribution, altitudinal data of the scalar electrical conductivity of the MA entry plasma are obtained and relevant MHD parameters, such as electron Hall parameter and ion slip coefficient were evaluated. Finally, the estimated MHD energy densities for the cases of an ideal and continuous Faraday generator are given in Figure 6.

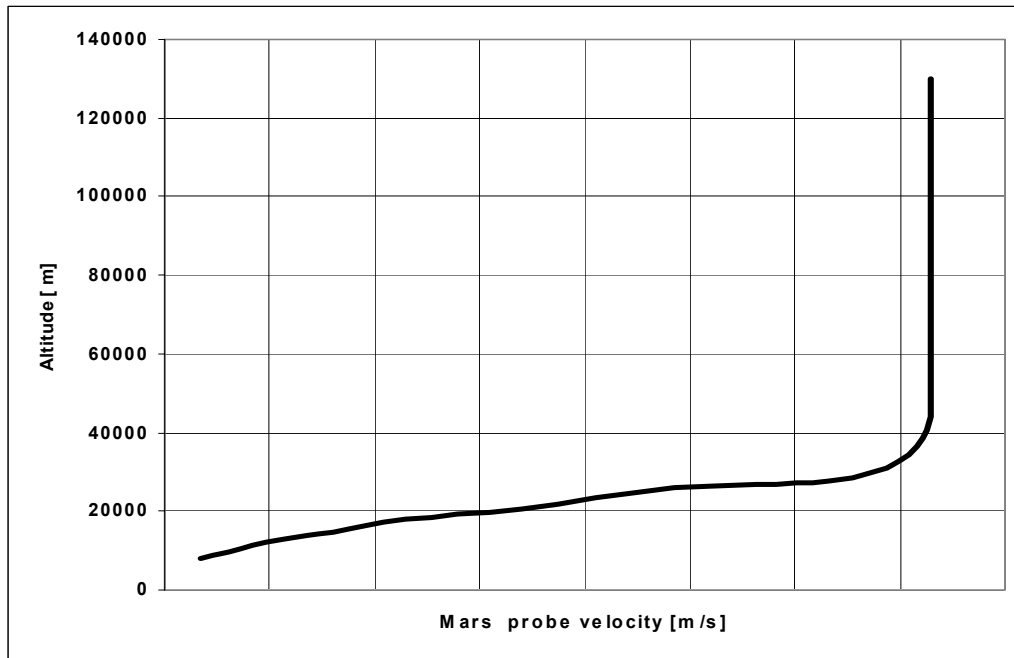


**Figure 1.** Altitudinal distribution of velocity of the Mars probe during the aero shell entry phase.

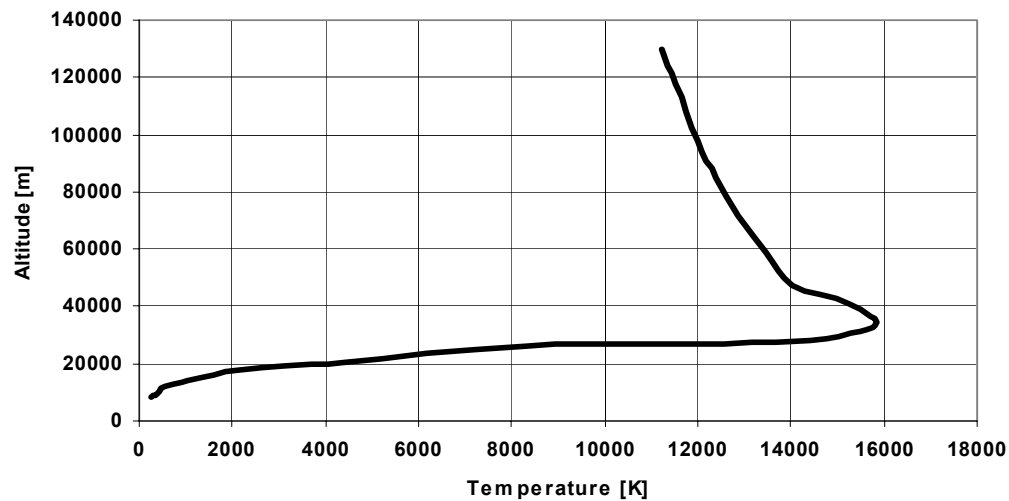


**Figure 2.** Altitudinal distribution of peak gas temperature in shock layer during the aerobraking phase of the Martian probe entry.

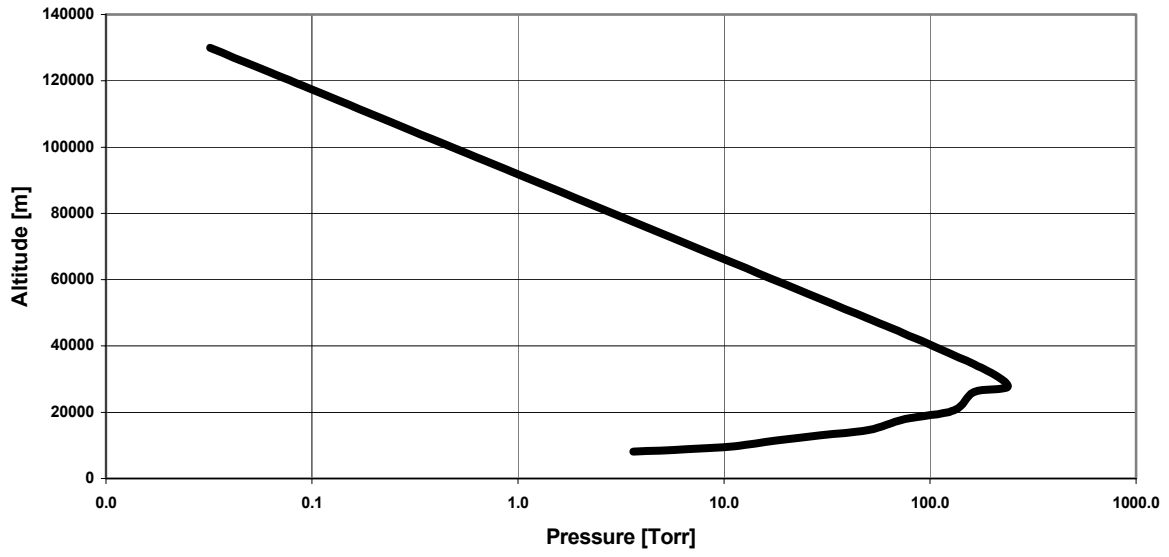


**Figure 3.** Altitudinal distribution of peak pressure in shock layer during the aerobreaking phase of the Martian probe entry.

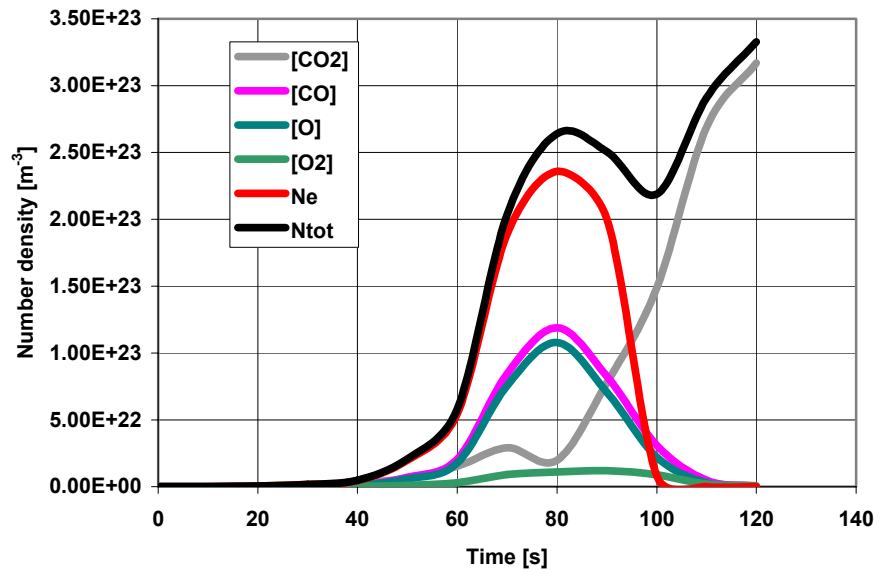


**Figure 4.** Time variation of total and partial number density of major constituents of the plasma generated during Martian probe entry.

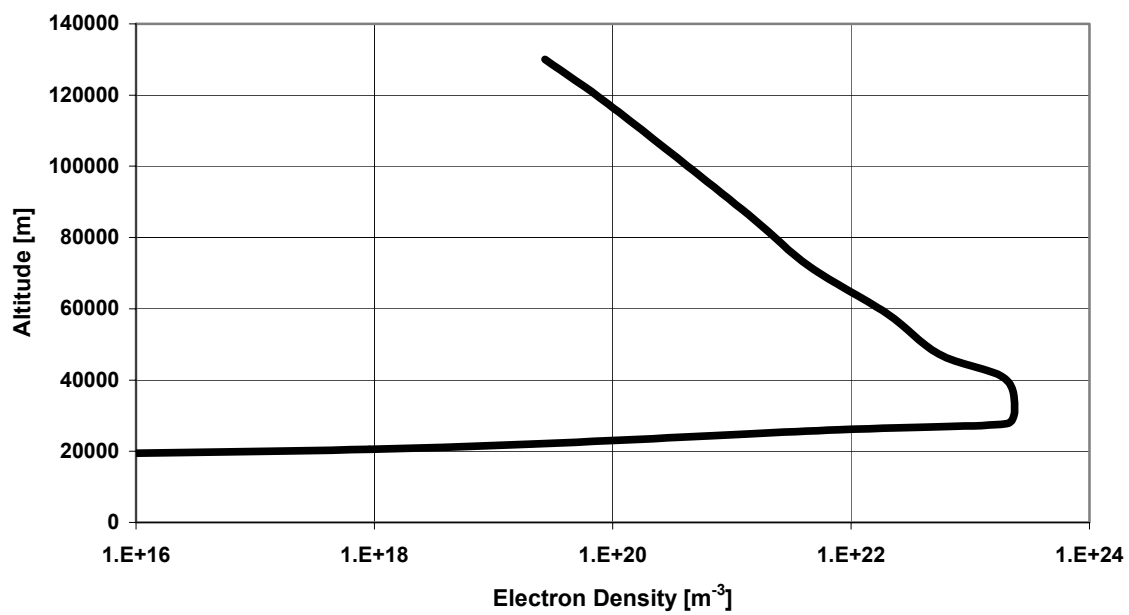


**Figure 5.** Electron density based on Saha equilibrium during Martian probe entry.

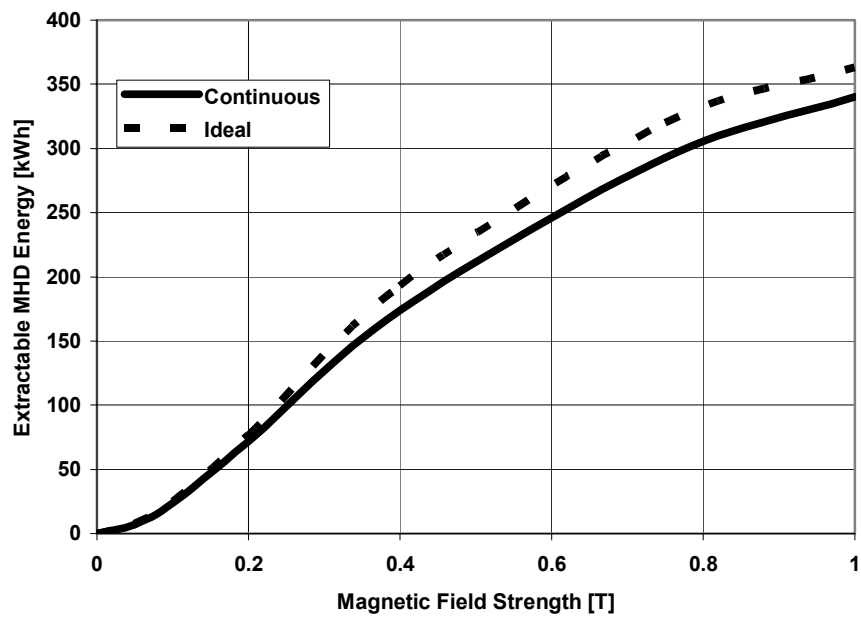


**Figure 6.** Extractable MHD energy from the Mars Pathfinder entry trajectory.

## Experiment

Experimental set up is a combination of supersonic flow tube and a microwave cavity discharge. Supersonic flow was generated with cylindrical convergent-divergent (De Laval) nozzle, shown schematically in Fig. 7. The nozzle was made of non-conductive microwave-transparent ceramics. Two O-rings provide separation between the upstream and downstream region. Nozzle was designed nominally for  $M = 3.5$  but actual measurements of stagnation and static pressure yielded  $M = 3.28$  in Martian simulant gas (95.7%  $\text{CO}_2$ , 2.7%  $\text{N}_2$ , and 1.6% Ar).

Test section is located downstream the discharge section of the tube. Flowing afterglow from the microwave cavity discharge provides the necessary ionization and conductivity. The specific feature of the microwave discharge used in our experiments is that it sustains high level of ionization relatively far away from the resonant cavity. In this configuration, quartz tube acts as microwave waveguide, that drives microwave field far into the test chamber, contrary to the d.c. flowing afterglow, where the external d.c. field is nonexistent outside the inter-electrode volume. Although we still call it flowing afterglow, in reality most of the ionization is sustained by the microwave field traveling along the tube. This is the enabling property that makes this discharge suitable for laboratory simulation of highly ionized Martian entry plasma.

An MHD generator containing electrodes and two permanent magnets is positioned downstream from the microwave cavity discharge. Model was connected to the feedthrough devices in the output section of the apparatus. Baratron pressure gauge monitored the static pressure in the test chamber. Output section consisted of diagnostic feedthrough devices, the roots blower, and two rotary mechanical pumps.

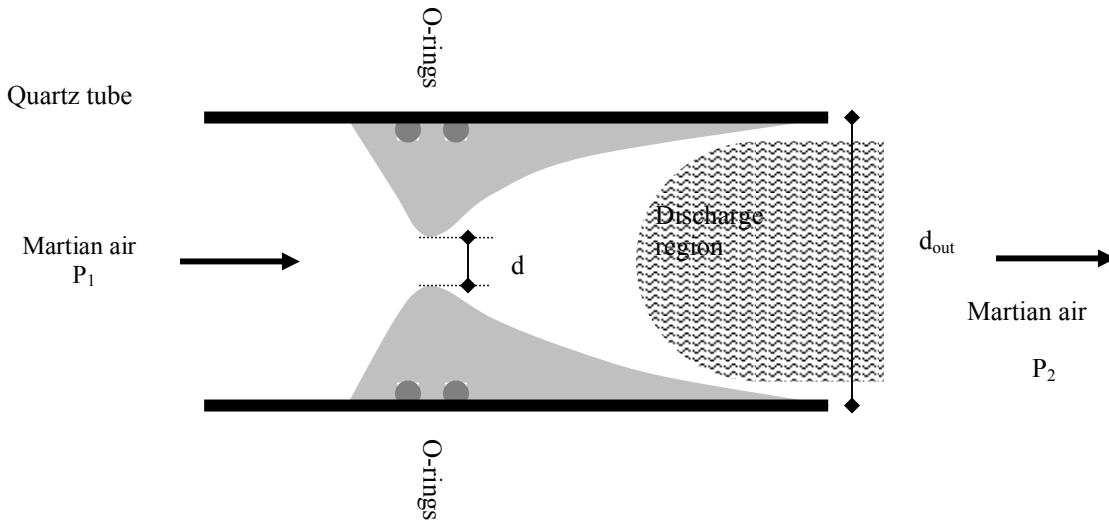


**Figure 7.** Scheme of the convergent-divergent (de Laval) nozzle showing direction of flow

## Flow Characteristics

Conventional optical methods for flow visualization could not be applied in the experiment since the static pressure in the tube is too low (1-3 Torr). Therefore we are searching for tools based on the optical emission spectroscopy. It was observed in the earlier work that the electronically excited states tend to accumulate at the location of the acoustic shock wave in weakly ionized gas. The aggregated populations of the electronically excited states are due to at least three factors: (a) collisional excitation of ground-state atoms; (b) cascade electro-ion recombination/deexcitation; and (c) resonant radiation trapping. We do not intend to go here into too much detail about the any of these mechanisms. Our goal is to explore the possibility to measure the standoff distance using the enhanced excited state population as the shock indicator. This was accomplished in Argon by measuring mostly the absolute intensities of spectral lines in the 4p-4s system along the flow axis, from the tip of the model to about 20

mm upstream of the model. For comparison some lines corresponding to higher energy levels (6s-4p, for instance) were also recorded. Scheme of the experiment is given in Fig. 8.

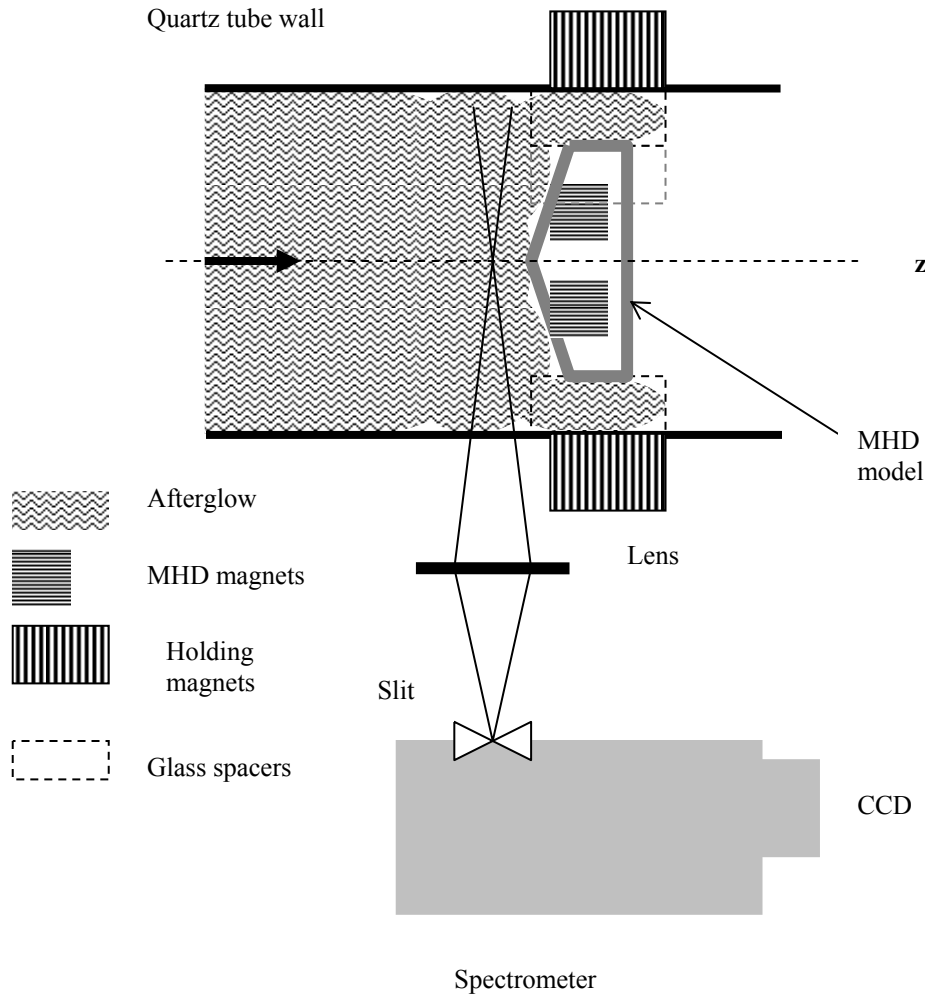


**Figure 8.** Scheme of the emission spectroscopy setup.

Emission spectra were recorded using a 0.5 m Acron monochromator with a 3600g/mm grating blazed at 240 nm, an 1800 g/mm grating blazed at 500 nm, and a 600 g/mm grating blazed at 300 nm. Detection system consisted of an Apogee spectral imaging camera with a Hamamatsu CCD detector (1024x256 pixels) and a Tektronix CCD detector (512x256 pixels). Wavelength was calibrated using a set of Spectra Physics Pen Lamps. Pixel/wavelength conversion factor was fitted using a third order polynomial recurrent formula separately for every grating used in recording spectra. Intensity was calibrated using the absolute blackbody irradiance source (Spectra Physics) separately for each grating/detector combination.

Model was positioned in the center of the quartz tube using three symmetrical glass spacers. Distribution of line intensity over z axis was measured by moving the model along z-axis using the external holding magnets. Each model position was measured with the ruler. Each line intensity was integrated from -50 to +50 pixels with respect to the line center. For the grating of 1800 grooves/mm this corresponded to the wavelength range of  $\pm 1$  nm. Baseline intensity was subtracted at every pixel using a self-made analysis software. Exposure time was kept constant so that it contains at least 5 successive MW plasma pulses.

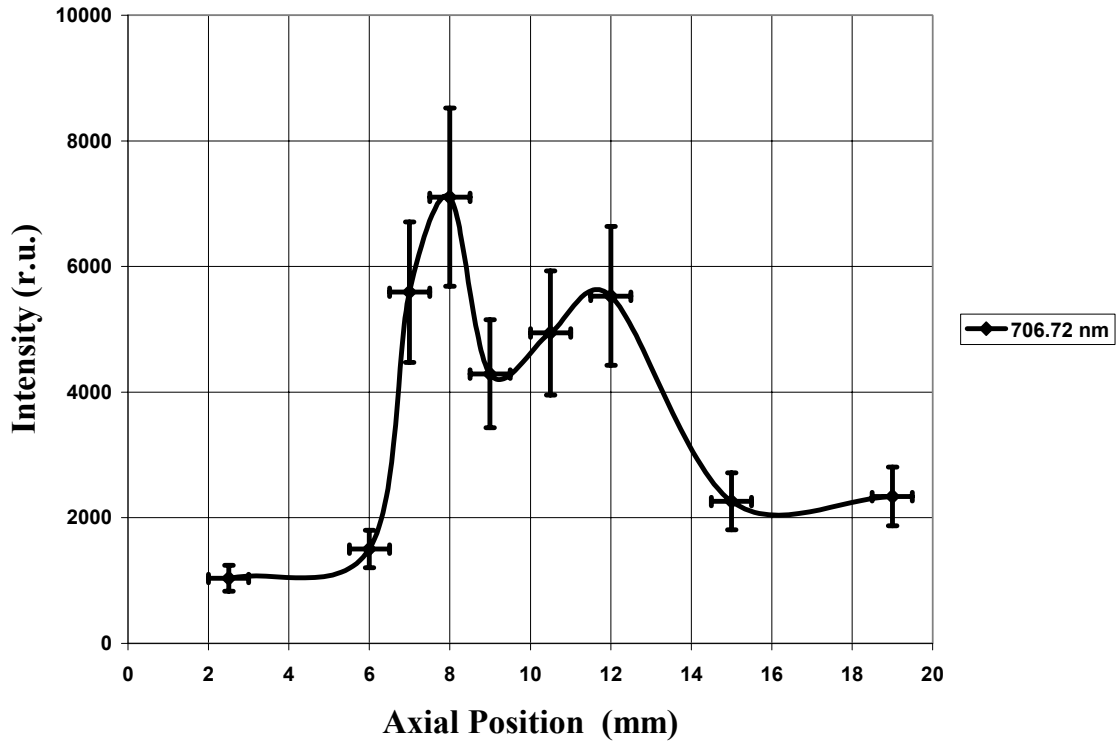


**Figure 9.** Axial distribution of spectral line ArI 706.72 nm (4p-4s). Tip of the model is at 0 mm.

More detailed study is required to generate a full quantitative correlation between the translational shock due to the model and the spectral line intensity distribution. However, we can state with confidence that the approximate standoff distance at the centerline of the flow is

$$\delta = 7.5 \text{ mm.}$$

In spherical approximation, where the model surface can be approximated with the effective spherical surface with  $R_{\text{body}} = 18.7 \text{ mm}$ , this value translates into

$$M = 1.7$$

which agrees with our estimate of the Mach number for the flow suppressed by the model.

## Plasma parameters

In order to verify the level of electron density produced by the microwave-induced supersonic afterglow, we added a small amount of Hydrogen into the stagnation chamber in order to measure spectral profiles of Hydrogen Balmer lines and derive two important parameters of the discharge plasma, the gas temperature from Doppler component, and the electron density from the Stark component of the line profile. Analysis of the Balmer line profile was discussed in [Orlando] and in the References therein. In Figure 3 we show the Voigt profile of the  $H_\gamma$  line in the microwave driven flowing afterglow at static pressure of 2 Torr. In this case, the ratio of Lorentz to Voigt halfwidth at half maximum (HWHM) was 0.4. The evaluated electron density is  $2.5 \times 10^{13} \text{ cm}^{-3}$ . Overall, in the static pressure range of interest here, the electron density was within  $1\text{--}3 \times 10^{13} \text{ cm}^{-3}$ .

From the Doppler component of the Voigt profile, after extraction of the instrumental profile, we obtain gas temperature of  $850^\circ \text{ K}$ , which is consistent with the fact that the Curie temperature was not reached, since both the external (holding) and internal magnets continued to operate normally during the tests.

## Current Calibration

Direct measurement of current collected by the model MHD power generator could be intrusive and lead to change in plasma conditions and could modify the values of measured parameters. Non-intrusive method, applied in this experiment relies on placing a light source (LED) diode into the circuit together with the model element and measure the light emitted from the diode, instead the current. This approach requires a separate measurements of LED diode emission characteristic. We define the LED diode emission characteristic as the relation between the current through the diode and light emission intensity. In present experiment light emission intensity was not measured in absolute values. We rather relied on the relative measurements where the geometry of the light detection was carefully controlled. Calibration was made by substituting the MHD generator with a high-impedance d.c. source with constant voltage, typically 3 V. A d.c. ammeter was connected in series with the resistor and LED diode. LED diode was placed at a fixed position in the light-proof housing together with the PMT detector. PMT signal was recorded on a digital oscilloscope with input impedance of 1 M $\Omega$ . Time constant of the recording circuit was of the order of 100  $\mu$ s and is not critical in this experiment, since pulse duration of a microwave discharge is longer than 1 ms. Resistance in the circuit was variable in order to change the current through the diode. Constant resistance of the LED diode was 200  $\Omega$ . Using the current-emission characteristic of the diode, the typical signal on the oscilloscope was as shown in Fig. 10. For comparison, a single pulse from the MW driving circuit is shown in arbitrary units, adjusted to scale of the diagram. One can notice that the actual collected current pulse is much shorter than the driving pulse, because the discharge breakdown conditions are met only at a certain level of microwave power and the inception of discharge plasma is lagging in time with respect to the onset of the microwave pulse. Current pulse is asymmetrical probably due to the additional time lag corresponding to the time of flight of the ionized gas. For instance, at 450 m/s the time of flight for the distance of 30 cm is 0.75 ms, which is slightly more than the time shift between the driving and the collected current pulse.

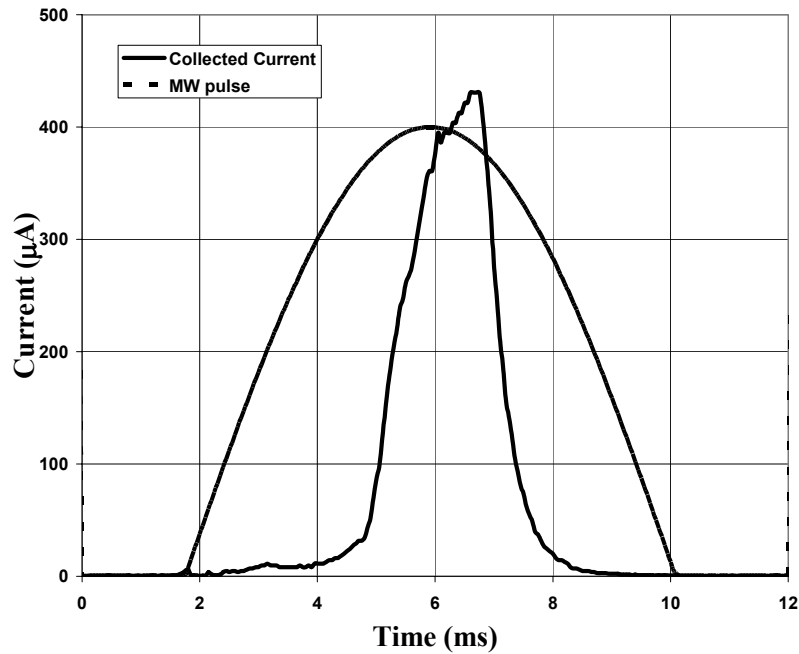


**Figure 10.** A typical MHD current pulse (unbiased) compared to an approximate MW pulse

## Conclusion

We have upgraded our microwave flowing afterglow apparatus so that it can produce supersonic flow in Martian simulant gas. Using a self-designed convergent-divergent nozzle we were able to generate flow velocity corresponding to  $M=3.28$  in the absence of model in the test chamber, at static pressure range of 0.5 to 3 Torr.



MHD generator model suppressed the flow so that the actual flow velocity was corresponding to an estimated value of  $M=1.7$ , based on the shock standoff distance at the centerline in spherical body approximation. This value is in a fair agreement with  $M=2$ , which is obtained from the analysis of the flow in the presence of the model.

Commercial microwave generator was used to sustain a cylindrical cavity discharge at power density between 3.5 and 7 W/cm<sup>3</sup>. The discharge was sustained downstream of the cavity by the traveling microwave field using the quartz tube as the wave guide. Therefore, this plasma generator differs from conventional d.c. flowing afterglow in the ability to sustain ionized gas over a longer distance. As a consequence, electron density is higher. Using the Stark broadening technique it was determined to be in the range of  $1-3 \times 10^{13}$  cm<sup>-3</sup>. Gas temperature from thermocouple measurements, Doppler component of the observed line profiles, and rotational spectra of nitrogen molecules was consistently lower or around 800 K with the average measurement error of 20%. The upper temperature limit affected the performance of the MHD generator model, but did not reach Curie point of permanent magnets of the model. Electron excitation temperature of argon 4p-4s lines was of the order of 2000 K.

Collected current of an unbiased model connected in series with the LED diode and 5000  $\Omega$  resistor, was between 0.3 and 1 mA, which is in fair agreement with the theoretical estimate given in the Appendix. When a 200 V bias was added into the circuit, the collected current increase 30 to 50 times. Maximum performance was obtained at about 5.5 W/cm<sup>3</sup>, which amounted to the peak current of 50 mA. This level of current allowed activation of at least 10 LED diodes in parallel connection. Unbiased model generated voltage of 3 V and was able to activate a Vertical Cavity Surface Emitting Laser (VCSEL).

Validation of MHD conversion concept in a supersonic microwave flowing afterglow apparatus, with an external MHD generator required an innovative diagnostic approach. Conventional optical methods for flow characterization could not be applied due to too low static pressure range (0.5-3 Torr). More elaborate modern optical techniques required equipment that was unavailable or underdeveloped. Therefore, we had to rely on optical emission spectroscopy not only to determine plasma parameters, but also to characterize the flow. Accumulation of electronically excited states near the shock layer and the consequent increase of spectral line intensity is a convenient effect for the development of a non-intrusive method for shock wave characterization in the flow of rarefied ionized gas. This fact has remained unnoticed due to the fact that most of the experiments in weakly ionized gas were performed using a traveling shock wave. Very few experiments on stationary shock have been reported so far, with less elaborate diagnostics.

Measurement of the collected current presented another challenge, especially in the case when bias was applied. Any direct measurement of electric parameters is at least intrusive if not outright impossible. Therefore, we opted for development of an optical-coupling technique, using the correlation between the current through a LED diode and the light emission. Absence of current threshold in the light source emission characteristics combined with the wide dynamic range of the PMT detector, allowed for the calibration of current over several orders of magnitude, from microampere to milliampere range.

## ACKNOWLEDGMENTS

This work was supported by NASA Langley Research Center under Contract No. L18716.

## REFERENCES

- Dinh, T., Thesis, Old Dominion University (2002), also: Vušković, L., R. L. Ash, Z. Shi, S. Popović, and T. Dinh, "Radio-Frequency-Discharge Reaction Cell for Oxygen Extraction from Martian Atmosphere," SAE Transactions, J. of Aerospace **106**, 1041 (1997).  
P. Bletzinger and B. N. Ganguly, Phys. Lett. A **258**, 342-345 (1999)  
S. Popović and L. Vušković, Physics of Plasmas **7**, 1448-51, (1999).